mathematics

IMPACT FACTOR 2.2

CITESCORE 4.6

Article

Local Quantum Uncertainty and Entanglement in the Hyperfine Structure of the Hydrogen Atom: A Lindblad Approach

Kamal Berrada and Smail Bougouffa

Special Issue
Advances in Mathematics for Quantum Mechanics

Edited by
Dr. L.S.F. Olavo

MDPI

https://doi.org/10.3390/math13203340

mathematics

MDPI

Article

Local Quantum Uncertainty and Entanglement in the Hyperfine Structure of the Hydrogen Atom: A Lindblad Approach

Kamal Berrada * and Smail Bougouffa

Department of Physics, College of Science, Imam Mohammad Ibn Saud Islamic University (IMSIU), P.O. Box 90950, Riyadh 11623, Saudi Arabia; sbougouffa@imamu.edu.sa
* Correspondence: kaberrada@imamu.edu.sa

Abstract

In this work, we investigate quantum correlations, including entanglement and quantum discord, within the hyperfine structure of the hydrogen atom using the Lindblad master equation to model its dynamics as an open quantum system interacting with an environment. By incorporating realistic environmental influences, we examine the time evolution of two key measures of quantum correlations: concurrence, which quantifies entanglement, and local quantum uncertainty (LQU), a broader indicator of quantumness. Our analysis spans various initial states, including coherent superpositions of hyperfine states, to capture a wide range of possible configurations and demonstrate how these measures capture distinct aspects of quantum behavior. The results reveal the robustness of LQU in regimes where entanglement may vanish. This resilience of LQU underscores its utility as a robust measure of quantum correlations beyond entanglement alone in the hydrogen atom. By elucidating the dynamics of quantum correlations in the hydrogen atom under realistic conditions, this work not only deepens our fundamental understanding of atomic systems but also highlights their potential relevance to quantum information science and the development of quantum technologies.

Keywords: Lindblad master equation; dephasing effect; hyperfine structure; hydrogen atom; quantum entanglement; local quantum uncertainty

MSC: 81P40; 81Q93; 81P45; 81S22

Academic Editor: L.S.F. Olavo

Received: 9 September 2025
Revised: 16 October 2025
Accepted: 17 October 2025
Published: 20 October 2025

Citation: Berrada, K.; Bougouffa, S. Local Quantum Uncertainty and Entanglement in the Hyperfine Structure of the Hydrogen Atom: A Lindblad Approach. *Mathematics* **2025**, *13*, 3340. https://doi.org/10.3390/math13203340

1. Introduction

Quantum entanglement, recognized as a hallmark of quantum mechanics since its foundational identification by Einstein, Podolsky, and Rosen in 1935, has emerged as a central concept in quantum information science. It underpins a wide array of quantum technologies, including quantum teleportation [1], quantum dense coding [2], quantum key distribution [3], and quantum computing [4]. As research in this field has matured, various quantitative measures of entanglement have been introduced to assess the strength and nature of quantum correlations. These include the relative entropy of the entanglement, the distillable entanglement, the concurrence, and negativity, among others [2,3,5–8]. Despite its fundamental role, entanglement has proven insufficient for characterizing all aspects of quantum correlations. It is now well established that quantum correlations can exist even in separable (non-entangled) states, indicating that the absence of entanglement does not imply purely classical behavior. In this context, quantum discord, introduced by Ollivier and Zurek in 2001 [9], provides a broader framework for capturing non-classical

correlations beyond entanglement. Based on differences between two classically equivalent definitions of mutual information, quantum discord reveals subtle quantum features using tools such as von Neumann entropy. The growing recognition that quantum discord and other non-classical correlations play critical roles in quantum tasks, sometimes even in the absence of entanglement, has driven extensive theoretical and experimental exploration. Recent studies have demonstrated that quantum discord can be a useful resource in various quantum protocols, including quantum communication, quantum metrology, and thermodynamics [6,10]. This has led to increased interest across a variety of physical platforms, from atomic and optical systems to condensed matter [11]. These developments emphasize the need for a deeper and more comprehensive understanding of quantum correlations as a foundation for future quantum technologies.

As a fundamental model for bound quantum systems, atomic hydrogen has played a pivotal role in the development of quantum mechanics. Its significance in early quantum theory is well documented and continues to serve as a cornerstone for modern physics research. The hydrogen atom remains an essential reference point for numerous physical studies, particularly through its hyperfine structure, which has facilitated advances in various fields. In recent years, research on the hyperfine structure of hydrogen has led to significant developments, including its application in the detection of dark matter [12–14], testing general relativity using hydrogen maser frequency standards [15], probing CPT symmetry within the Standard Model of elementary particle physics [16,17], and advancing quantum computing by enabling quantum registers [18]. These diverse applications highlight the continuing relevance of hydrogen in contemporary physics, offering a bridge between foundational quantum mechanics and emerging technologies. Despite extensive research on quantum systems, a comprehensive understanding of quantum correlations in hydrogen atoms, particularly in the context of open-system dynamics and decoherence, remains a topic of active investigation. Studying these phenomena is crucial for assessing the robustness of quantum correlations and their potential applications in quantum information processing and related technologies.

Realistic quantum systems are inherently vulnerable to decoherence and noise from their external environments, putting a risk on critical quantum resources such as entanglement and quantum discord, both essential for quantum computing and information processing [19]. To address these challenges, researchers have developed various strategies, including quantum error correction codes [20], and dynamical decoupling [21], to enhance the resilience of quantum states. Recent advances have explored engineered environments and quantum control techniques to mitigate noise, with some approaches leveraging collective protective effects within an enlarged Hilbert space to dilute the noise coupling strength per qubit [22]. Furthermore, the role of non-Markovian structured environments, characterized by memory effects and temporal correlations, has been extensively studied for their potential to preserve quantum entanglement and parameter estimation [23]. Various strategies have been proposed to mitigate decoherence, including dynamical decoupling, reservoir engineering, non-Markovian control [24,25], quantum Zeno effect [26,27], and quantum-jump-based feedback [28]. More recently, studies are continuing to refine these hybrid approaches, combining environmental engineering with quantum error correction to enable scalable quantum technologies [29]. In this work, we adopt the Lindblad master equation [30] to describe the dynamics of the hydrogen hyperfine system. It should be noted that the Lindblad formalism provides a Markovian approximation of open-system dynamics, and thus represents a specific class of environments rather than a fully general framework.

In the present manuscript, we plan to investigate quantum correlations, including entanglement and LQU dynamics, within the hyperfine structure of the hydrogen atom using the Lindblad master equation to model its dynamics as an open quantum system

interacting with an environment. Such exploration offers several significant advantages. First, the hydrogen atom is one of the most fundamental and precisely understood quantum systems, making it an ideal platform for studying quantum correlations and decoherence in a controlled and analytically tractable setting. The hyperfine interaction naturally creates a bipartite spin system, electron and proton, allowing for a clear investigation of the dynamics of entanglement and LQU. Second, the Lindblad technique provides a systematic and physically consistent framework for modeling open quantum systems, ensuring that the evolution remains completely positive and trace-preserving, which is essential when accounting for environmental effects. This allows for a realistic and quantitative analysis of how quantum entanglement and LQU degrade over time. Finally, by applying the quantumness measures within this framework, one can uncover subtle distinctions between different types of quantum correlations, entanglement versus LQU [31,32], thus gaining a deeper understanding of the quantum features that can persist even when the entanglement vanishes. This has implications for quantum information processing, quantum thermodynamics, and fundamental studies of decoherence.

This manuscript is organized as follows. In Section 2, we investigate the hyperfine model of the hydrogen atom. Furthermore, we present the evolution of the hydrogen density matrix within the framework of the Lindblad formalism. Section 3 introduces and analyzes two key measures, concurrence and LQU, to investigate the quantum dynamics of entanglement and discord. These measures are applied across a variety of initial conditions, specifically coherent superpositions of hyperfine states, to assess the evolution of quantum correlations under the Lindblad framework. Section 4 displays the time evolution of quantumness measures used in the analysis and provides a discussion of the results. The comparative analysis reveals the distinct sensitivities of the concurrence and LQU, offering complementary perspectives on how entanglement and more general quantum correlations manifest themselves in different configurations of the system. Finally, Section 5 concludes the paper with comments and a summary of the results.

2. Hyperfine Interaction in Hydrogen and Lindblad Formalism

In the hydrogen atom, the hyperfine interaction couples the electron spin to the nuclear spin. The ground-state electron ($1s$ orbital) possesses no orbital angular momentum ($\ell = 0$), which eliminates any magnetic field in the nucleus originating from orbital motion. Consequently, the hyperfine interaction arises solely from the magnetic dipole coupling between the intrinsic spins of the electron and proton [33]. The measured hyperfine splitting corresponds to a transition frequency of 1420 MHz (the 21 cm line), a result of this spin–spin interaction [34]. Theoretical calculations employing first-order perturbation theory for the magnetic dipole interaction between the electron and nucleus account for the coupling strength of the $\mathbf{I} \cdot \mathbf{S}$ term, where $\mathbf{I}$ and $\mathbf{S}$ denote the nuclear and electron spin operators, respectively. When an external magnetic field is incorporated, the system's Hamiltonian expands to include both the hyperfine coupling and Zeeman interactions [34–36].

The effective Hamiltonian for the ground-state hyperfine structure of atomic hydrogen is given by the following:

$$H_{\mathrm{HF}} = J\hat{\boldsymbol{\sigma}}_{\boldsymbol{e}} \cdot \hat{\boldsymbol{\sigma}}_{\boldsymbol{p}} = J\left(\sigma_x^e \sigma_x^p + \sigma_y^e \sigma_y^p + \sigma_z^e \sigma_z^p\right), \tag{1}$$

where J is the hyperfine coupling constant, and $\hat{\boldsymbol{\sigma}}_{\boldsymbol{e}}$ and $\hat{\boldsymbol{\sigma}}_{\boldsymbol{p}}$ are the Pauli operators for the electron and proton, respectively.

The coupling constant J is explicitly expressed as [34]

$$J = \frac{2\pi}{3} \frac{1}{4\pi\varepsilon_0} \frac{g_e e}{2m_e} \frac{g_p e}{2m_p} \frac{\hbar^2}{c\pi a_0^3}, \tag{2}$$

where ε_0 is the vacuum permittivity, $\hbar$ is the reduced Planck's constant, c is the speed of light, a_0 is the Bohr radius, g_e and g_p are the g-factors for the electron and proton, respectively, and m_e and m_p are the electron and proton masses, respectively. This formula encapsulates the magnetic interaction strength, derived from the electron's wavefunction density at the nucleus.

We assume that the two-dimensional Hilbert space that describes the electron spin is generated by the basis vectors representing the spin-up and spin-down states, expressed as $\{|\uparrow_e\rangle, |\downarrow_e\rangle\}$, while the proton spin occupies a two-dimensional Hilbert space defined by its own spin-up and spin-down basis vectors, given by $\{|\uparrow_p\rangle, |\downarrow_p\rangle\}$. Consequently, the hyperfine structure of the hydrogen atom resides in a four-dimensional Hilbert space, with a basis formed by the tensor product of these states, written as $\mathcal{B} = \{|\uparrow_e\uparrow_p\rangle, |\uparrow_e\downarrow_p\rangle, |\downarrow_e\uparrow_p\rangle, |\downarrow_e\downarrow_p\rangle\}$. In this basis, the Hamiltonian yields the following eigenvalues and eigenvectors: the singlet state with eigenvalue $E_a = -3J$ and eigenstate $|a\rangle = \frac{1}{\sqrt{2}}(|\uparrow_e\downarrow_p\rangle - |\downarrow_e\uparrow_p\rangle)$; three triplet states with eigenvalue $E_b = E_c = E_d = J$, with eigenstates $|b\rangle = |\uparrow_e\uparrow_p\rangle$, $|c\rangle = \frac{1}{\sqrt{2}}(|\uparrow_e\downarrow_p\rangle + |\downarrow_e\uparrow_p\rangle)$, and $|d\rangle = |\downarrow_e\downarrow_p\rangle$.

The eigenvalues $E_a, E_b = E_c = E_d$ correspond to the singlet and triplet states of the hyperfine structure. Consequently, the quantum ground state of the system is identified as the singlet state $|a\rangle$, characterized by its energy eigenvalue E_a. Hyperfine energy splitting ΔE—defined as the energy difference between the singlet states ($|a\rangle$) and triplet states—emerges from the exchange interaction $\Delta E = 4J \approx 5.88$ μeV. Under an external magnetic field [36], this splitting becomes field-dependent, and the ground state evolves from a Bell state of maximum intrusion into a field-dependent configuration. Such behavior is critical for applications in precision spectroscopy and quantum technologies.

To explore the time evolution of the electron–proton state in the context of hyperfine structure, we propose employing the Lindblad formalism, a modified extension of the Schrödinger equation [11]. This model introduces a decoherence factor to account for phase decoherence in a Markovian environment, providing a practical framework to study the robustness and evolution of quantum correlations in a dynamically expanding universe. The Lindblad formalism offers several advantages in analyzing the dynamics of entanglement in the hyperfine structure of the hydrogen atom. It captures phase decoherence by introducing an intrinsic mechanism that modifies the unitary evolution of quantum states, enabling the assessment of how robust or fragile the entanglement and discord is under realistic conditions. Furthermore, it provides a powerful framework for exploring the persistence and degradation of quantum correlations in hydrogen's internal spin degrees of freedom. By modeling deviations from idealized unitary dynamics, particularly through extensions such as the Milburn model, the Lindblad approach offers a means to investigate the emergence of classical behavior in quantum systems influenced by environmental noise. To model the hyperfine structure using the Lindblad approach, we consider the evolution of the density matrix $\rho(t)$ under the influence of decoherence. The following equation describes the Lindblad model [37–39]:

$$\frac{d\rho(t)}{dt} = -\frac{i}{\hbar}[H_{\mathrm{HF}}, \rho(t)] + \frac{\gamma}{2}\sum_k \left(L_k \rho(t) L_k^\dagger - \frac{1}{2}\{L_k^\dagger L_k, \rho(t)\} \right), \tag{3}$$

where H_{HF} is the hyperfine Hamiltonian,γ is the decoherence rate, and L_k represents Lindblad operators that in turn represents environmental interactions. The first term accounts for unitary evolution due to the hyperfine interaction, while the second term models decoherence, assuming a Markovian environment where interactions are memoryless. It is worth noting that the Hamiltonian H_{HF} given in Equation (1) corresponds formally to the isotropic Heisenberg XXX model. Consequently, the Lindblad master equation in Equation (3) may be viewed as a particular case of the general spin–spin

interaction model, akin to the infinite-temperature limit discussed in Ref. [40]. However, unlike the N-qubit XY system coupled to thermal and dephasing reservoirs studied in that work, the present model describes a physically distinct situation—namely the hyperfine interaction between the electron and proton in a hydrogen atom, forming an intrinsic two-qubit system coupled through exchange interaction.

For the hyperfine structure, decoherence is modeled via spin-flip processes and affects the electron and proton spins. The Lindblad operators are defined as follows:

$$\begin{aligned} L_1 &= \sigma_+^e \otimes I_p, \quad \text{(electron excitation, } |\downarrow_e\rangle \to |\uparrow_e\rangle\text{)}, \\ L_2 &= \sigma_-^e \otimes I_p, \quad \text{(electron relaxation, } |\uparrow_e\rangle \to |\downarrow_e\rangle\text{)}, \\ L_3 &= I_e \otimes \sigma_+^p, \quad \text{(proton excitation, } |\downarrow_p\rangle \to |\uparrow_p\rangle\text{)}, \\ L_4 &= I_e \otimes \sigma_-^p, \quad \text{(proton relaxation, } |\uparrow_p\rangle \to |\downarrow_p\rangle\text{)}, \end{aligned} \tag{4}$$

where the Pauli ladder operators are given by

$$\sigma_+ = \begin{bmatrix} 0 & 1 \\ 0 & 0 \end{bmatrix}, \quad \sigma_- = \begin{bmatrix} 0 & 0 \\ 1 & 0 \end{bmatrix}, \tag{5}$$

and I_e and I_p are identity operators for the electron and proton, respectively. These operators facilitate transitions between the spin states of the electron and proton within the hydrogen atom's hyperfine structure. This approach provides a transparent physical picture of how coherence and entanglement evolve under the combined influence of the hyperfine interaction and environmental spin-flip noise.

In our model, the four Lindblad operators (L_k) represent spin-flip processes affecting the electron and proton spins of the hydrogen atom. Physically, such processes can arise from several sources, including thermal fluctuations of the surrounding electromagnetic field, stray or fluctuating magnetic fields, and radiative coupling to vacuum modes. While we do not model a specific environment, this phenomenological approach captures the essential decoherence mechanisms affecting spin dynamics within a Markovian framework.

On the other hand, in the present study, we focus on spin-flip (relaxation/excitation) processes as the primary source of decoherence for the hydrogen hyperfine system. These processes directly affect the populations of the spin states and therefore have a significant impact on both concurrence and LQU. Pure dephasing, in contrast, influences only the off-diagonal elements of the density matrix without changing populations. While dephasing is relevant in certain physical situations, such as low-temperature environments with negligible energy exchange, spin-flip processes are typically dominant in realistic atomic systems interacting with fluctuating electromagnetic fields, random magnetic fields, or thermal reservoirs. The Lindblad formalism allows, in principle, the inclusion of both spin-flip and dephasing channels simultaneously. For clarity and tractability, we have chosen to focus on spin-flip processes in this work, as they provide a clear and illustrative picture of the dynamics of quantum correlations under population-altering decoherence. Extensions including pure dephasing can be considered in future work.

Expanding the Lindblad equation (3) with the basis $\mathcal{B} = \{|1\rangle = |\uparrow_e\uparrow_p\rangle, |2\rangle = |\uparrow_e\downarrow_p\rangle, |3\rangle = |\downarrow_e\uparrow_p\rangle, |4\rangle = |\downarrow_e\downarrow_p\rangle\}$, we obtain coupled differential equations for the matrix elements $\rho_{ij}(t)$. The evolution equations for the diagonal elements are

$$\begin{aligned}
\frac{d}{dt}\rho_{11}(t) &= \gamma(\rho_{33}(t) + \rho_{22}(t) - 2\rho_{11}(t)),\\
\frac{d}{dt}\rho_{22}(t) &= -i2G(\rho_{32}(t) - \rho_{23}(t)) + \gamma(\rho_{44}(t) + \rho_{11}(t) - 2\rho_{22}(t)),\\
\frac{d}{dt}\rho_{33}(t) &= -i2G(\rho_{23}(t) - \rho_{32}(t)) + \gamma(\rho_{44}(t) + \rho_{11}(t) - 2\rho_{33}(t)),\\
\frac{d}{dt}\rho_{44}(t) &= \gamma(\rho_{22}(t) + \rho_{33}(t) - 2\rho_{44}(t)),
\end{aligned} \tag{6}$$

where $G = J/\hbar$. For the off-diagonal elements, we obtain

$$\begin{aligned}
\frac{d}{dt}\rho_{12}(t) &= -i2G(\rho_{12}(t) - \rho_{13}(t)) + \gamma(\rho_{34}(t) - 2\rho_{12}(t)),\\
\frac{d}{dt}\rho_{13}(t) &= -i2G(\rho_{13}(t) - \rho_{12}(t)) + \gamma(\rho_{24}(t) - 2\rho_{13}(t)),\\
\frac{d}{dt}\rho_{14}(t) &= -2\gamma\rho_{14}(t),\\
\frac{d}{dt}\rho_{23}(t) &= -i2G(\rho_{33}(t) - \rho_{22}(t)) - 2\gamma\rho_{23}(t),\\
\frac{d}{dt}\rho_{24}(t) &= -i2G(\rho_{34}(t) - \rho_{24}(t)) + \gamma(\rho_{13}(t) - 2\rho_{24}(t)),\\
\frac{d}{dt}\rho_{34}(t) &= -i2G(\rho_{24}(t) - \rho_{34}(t)) + \gamma(\rho_{12}(t) - 2\rho_{34}(t)),
\end{aligned} \tag{7}$$

along with their complex conjugates. These equations describe how populations transfer between states and how coherences decay due to environmental interactions.

For an initial state representing a coherent superposition [41], such as

$$|\psi\rangle = \cos(\alpha)|\uparrow_e\downarrow_p\rangle + \sin(\alpha)|\downarrow_e\uparrow_p\rangle, \tag{8}$$

the density matrix evolves according to the Lindblad equation. This state is particularly relevant as it allows for tunable entanglement by varying the mixing angle α, with $\alpha = \pi/4$ yielding a maximally entangled state. In the analysis, α is treated as a fixed parameter for each specific case, while it can be varied across different scenarios to explore how the degree of initial entanglement affects the subsequent dynamics. Analytical solutions for this state yield

$$\begin{aligned}
\rho_{11}(t) &= \frac{1}{4}\left[1 - e^{-4\gamma t}\right],\\
\rho_{44}(t) &= \frac{1}{4}\left[1 - e^{-4\gamma t}\right],\\
\rho_{22}(t) &= \frac{1}{4}\left[1 + e^{-4\gamma t} + 2\cos(2\alpha)\cos(4Gt)e^{-2\gamma t}\right],\\
\rho_{33}(t) &= \frac{1}{4}\left[1 + e^{-4\gamma t} - 2\cos(2\alpha)\cos(4Gt)e^{-2\gamma t}\right],\\
\rho_{23}(t) &= \frac{1}{2}e^{-2\gamma t}[i\cos(2\alpha)\sin(4Gt) + \sin(2\alpha)],\\
\rho_{ij}(t) &= 0 \quad \text{for all other } i, j,
\end{aligned} \tag{9}$$

illustrating the decay of coherences and redistribution of populations over time. These solutions highlight the interplay between coherent oscillations (driven by G) and decoherence (governed by γ).

With the analytical expressions of the time-evolved density matrix at hand, we are now equipped to investigate various measures of quantum correlations that emerge in the hyperfine dynamics of the hydrogen atom. These expressions provide the necessary framework to compute key quantities such as concurrence and local quantum uncertainty.

In the following sections, we utilize these results to explore how quantum correlations of the electron–proton state evolve under the influence of decoherence in the framework of the hyperfine interaction.

3. Quantum Correlation Measures for Hyperfine Structure Dynamics

To explore the non-classical characteristics found in the hyperfine structure of atomic systems using an open quantum dynamics framework, we utilize two complementary measures of quantum correlations. The first measure is concurrence, which reflects the inherent entanglement between subsystems and is especially useful for characterizing the correlations of pure states and their decay through decoherence. The second measure is a discord-like metric, specifically the local quantum uncertainty (LQU), which evaluates quantum correlations based on the irreducible disturbance caused by local observables. Unlike measures of entanglement, the LQU is sensitive to a wider range of non-classical correlations, including those found in separable mixed states. We apply both measures within the framework of a Lindblad master equation that models the dissipative dynamics of the hyperfine levels, with the goal of identifying the dynamical behavior of quantum correlations.

3.1. Concurrence

Quantifying entanglement is essential for understanding how quantum systems, such as the hyperfine structure of the hydrogen atom, behave under environmental decoherence. Among various entanglement measures, concurrence, introduced by Wootters [5], is widely used for two-qubit systems due to its computational simplicity and direct relation to the entanglement of formation.

For a two-qubit system described by a density matrix ρ, the concurrence $C(\rho)$ is defined as follows [5,42–49]:

$$C(\rho) = \max\{0, \sqrt{\varepsilon_1} - \sqrt{\varepsilon_2} - \sqrt{\varepsilon_3} - \sqrt{\varepsilon_4}\}. \tag{10}$$

Here, ε_i are the eigenvalues, arranged in descending order, of the matrix

$$R = \sqrt{\rho}\tilde{\rho}\sqrt{\rho}, \tag{11}$$

where $\tilde{\rho}$ is the density matrix, defined as

$$\tilde{\rho} = (\hat{\sigma}_y \otimes \hat{\sigma}_y)\rho^*(\hat{\sigma}_y \otimes \hat{\sigma}_y), \tag{12}$$

with ρ^* representing the complex conjugate of ρ, and $\hat{\sigma}_y$ being the Pauli y operator, commonly used in quantum mechanics to describe spin or polarization states. Concurrence, denoted as $C(t)$, quantifies entanglement: $C(t) = 0$ corresponds to a separable (un-entangled) state, $C(t) = 1$ signifies maximal entanglement, and values in the range $0 < C(t) < 1$ describe partially entangled states.

With the density matrix with an evolution in time $\rho(t)$ given by nonzero elements and all other components that disappear as defined in Equation (9), the structure of $\rho(t)$ reflects a block-diagonal form where coherence exists only between the states $|\uparrow_e\downarrow_p\rangle$, $|\downarrow_e\uparrow_p\rangle$. This allows us to simplify the computation of entanglement measures. Substituting the corresponding density matrix elements into the standard definition of concurrence for an X-type two-qubit state, we obtain

$$C(t) = 2\max\{0, |\rho_{23}(t)| - \sqrt{\rho_{11}(t)\rho_{44}(t)}\}. \tag{13}$$

This expression can be conveniently rewritten as

$$C(t) = \max\{0,\, c(t)\}, \tag{14}$$

$$c(t) = e^{-2\gamma t}\sqrt{1-\cos^2(2\alpha)\cos^2(4Gt)} + \tfrac{1}{2}\left(e^{-4\gamma t}-1\right). \tag{15}$$

Equation (13) quantifies the interplay between quantum coherence, represented by the off-diagonal element $|\rho_{23}(t)|$, and population mixing, described by the diagonal terms $\rho_{11}(t)$ and $\rho_{44}(t)$. The time evolution of the concurrence is thus determined by the combined effects of dissipation (γ), spin–spin interaction strength (G), and the initial state mixing angle (α), revealing how coherence loss and coupling dynamics compete in shaping the entanglement behavior.

3.2. *Quantifying Quantum Correlations via Local Observables*

Quantum discord captures the presence of nonclassical correlations in a state that go beyond entanglement and is fundamentally characterized by the absence of quantum-certain local observables. In this context, the quantity $\mathcal{U}_A^{\Lambda}(\rho)$ introduced in [50], known as the local quantum uncertainty (LQU), functions not only as an indicator but as a proper *measure* of quantum correlations between subsystems (A and B) [51].

A central tool in our analysis is the LQU [50], defined as the minimal Wigner–Yanase skew information associated with a single local von Neumann measurement. For a bipartite state $\rho \equiv \rho_{AB}$ and a local observable $K^{\Lambda} = K_A^{\Lambda} \otimes \mathbb{I}_B$, where K_A^{Λ} is Hermitian with a nondegenerate spectrum Λ, the LQU with respect to subsystem A reads

$$\mathcal{U}_A^{\Lambda}(\rho) \equiv \min_{K^{\Lambda}} \mathcal{I}(\rho, K^{\Lambda}). \tag{16}$$

This defines a family of Λ-dependent measures, each corresponding to a class of maximally informative local observables on A. Practically, K_A^{Λ} can be written as $K_A^{\Lambda} = V_A\,\mathrm{diag}(\Lambda)\,V_A^{\dagger}$, where V_A varies over the special unitary group on A, and Λ sets the measurement scale, while V_A determines the measurement basis. For any non-degenerate observable Λ, the LQU rigorously fulfills all the established criteria required of a discord-like measure [6,50]: it is invariant under local unitary transformations, nonincreasing under local operations on subsystem B, vanishes if and only if the state has zero discord with respect to measurements on A, and reduces to an entanglement monotone in the case of pure states.

For bipartite systems of the form $2 \times d$, the LQU stands out for its practicality. Unlike most discord measures, which involve complex optimizations that are often intractable, even for two qubits [6,52–54], the LQU admits an explicit closed-form solution for any qubit–qudit state $\rho_{AB} \in \mathbb{C}^2 \otimes \mathbb{C}^d$. Furthermore, for a qubit A, all Λ-dependent versions are equivalent up to a constant factor [50]. We therefore drop the superscript and fix nondegenerate observables of the form $K_A = V_A \sigma_z V_A^{\dagger} = \vec{n}\cdot\vec{\sigma}_A$, with $|\vec{n}| = 1$, which ensures normalization to unity for maximally entangled pure states. Equation (16) then simplifies to

$$\mathcal{U}_A(\rho_{AB}) = 1 - \lambda_{\max}(Z_{AB}), \tag{17}$$

where $\lambda_{\max}$ is the maximal eigenvalue of the 3×3 symmetric matrix Z_{AB} with elements

$$(Z_{AB})_{ij} = \mathrm{Tr}\left\{\rho_{AB}^{1/2}(\sigma_i^A \otimes \mathbb{I}_B)\,\rho_{AB}^{1/2}(\sigma_j^A \otimes \mathbb{I}_B)\right\},$$

for $i, j = x, y, z$. In the case of pure states $|\psi_{AB}\rangle\langle\psi_{AB}|$, Equation (17) reduces to the linear entropy of entanglement, $\mathcal{U}_A(|\psi_{AB}\rangle\langle\psi_{AB}|) = 2(1 - \mathrm{Tr}\rho_A^2)$, where ρ_A is the marginal state of subsystem A. LQU in the 1 vs. n qubit partition has been shown [50] to match the scaling behavior of the canonical discord measures [9,53]. Beyond its analytic tractability, the

LQU offers a physically meaningful interpretation of discord, as the minimum quantum contribution to the statistical variance of local observables in a correlated state.

4. Results and Analysis

To analyze the robustness of quantum correlations for the hyperfine structure of the hydrogen atom in the presence of environmental decoherence, we display the time evolution of concurrence and LQU with respect the model parameters. These quantities are evaluated for initialization in a maximally entangled NOON state (8) and evolved using the Lindblad master equation.

Figure 1 illustrates the time evolution of quantum correlations, concurrence and LQU, as functions of dimensionless time Gt for different values of the relative decay factor γ, introduced through the Lindblad formalism. The solid black, dashed red, and dotted-dashed blue lines correspond to $\gamma = 0.05G$, $\gamma = 0.1G$, and $\gamma = 0.5G$, respectively. These results are obtained for the hyperfine structure of the hydrogen atom, assuming an initial maximally entangled NOON state and evolving under Lindblad-type open system dynamics. In the concurrence plot, entanglement decays faster with increasing γ, and for larger values such as $\gamma = 0.5G$, it vanishes abruptly, exhibiting entanglement sudden death (ESD). From the expression (13) of the concurrence evaluated for the initially maximally entangled NOON state, we can identify the sudden death onset of the entanglement, an abrupt vanishing of the entanglement in finite time due to decoherence. By setting the concurrence $C(t)$ to zero and solving for the time t, we obtain an analytical expression for the entanglement sudden death time, given by

$$t_s = -\frac{1}{2\gamma} \ln\left(\frac{\sqrt{2}-1}{2}\right). \tag{18}$$

The result highlights the fragility of entanglement under dissipative dynamics and quantifies how the decay rate γ governs the lifetime of quantum correlations. It also emphasizes the importance of identifying quantum states and environments that preserve entanglement over longer timescales, which is critical for practical applications in quantum information processing. In contrast, the LQU plot shows that quantum correlations beyond entanglement decay asymptotically and do not exhibit sudden death, even under strong decoherence. This contrast emphasizes that while entanglement is highly fragile under environmental influence, more general quantum correlations captured by LQU can persist, making them more robust indicators of quantumness in open quantum systems.

In our simulations, the decoherence rate γ is expressed relative to the coherent coupling strength G, with representative ratios $\gamma/G = 0.05, 0.1$, and 0.5. These values were selected to explore different dynamical regimes of the open quantum system, ranging from weak to moderate decoherence. In the context of hyperfine transitions in hydrogen, γ can be interpreted as an effective rate associated with spin relaxation or magnetic field fluctuations that perturb the electron–proton spin coupling. Although the precise value of γ depends on the surrounding environment (e.g., temperature, magnetic field noise, or residual radiation coupling), theoretical estimates for spin–decoherence times in atomic systems typically yield $\gamma/G \lesssim 1$, consistent with the range considered here. Hence, these ratios are not meant to represent a specific experimental configuration but rather to capture the qualitative transition between coherent and decoherence-dominated dynamics.

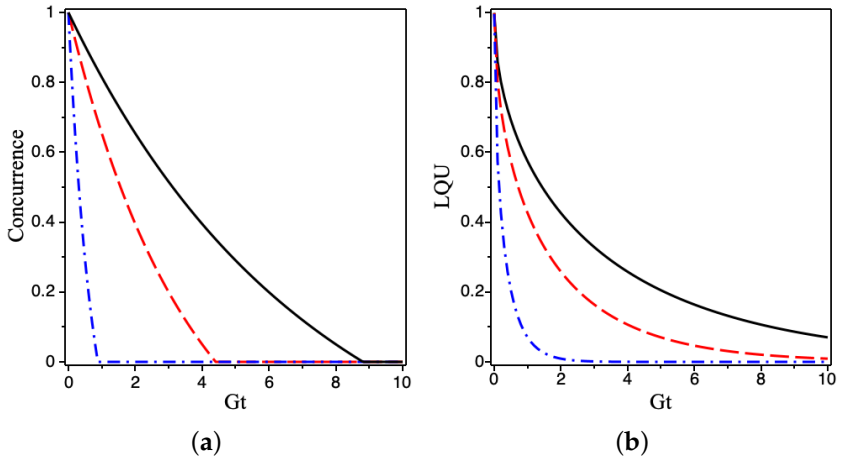

Figure 1. Time evolution of the concurrence $C(t)$ (**a**), and the local quantum uncertainty LQU (**b**) as a function of time t for the coherent superposition of hyperfine state $\cos(\alpha)\,|\uparrow_e\downarrow_p\rangle + \sin(\alpha)\,|\downarrow_e\uparrow_p\rangle$, $\alpha = \frac{\pi}{4}$ for different values of γ. Solid black: $\gamma = 0.05G$; dashed red: $\gamma = 0.1G$; dotted–dashed blue: $\gamma = 0.5G$.

In Figure 2, we show the dynamical behavior of quantum concurrence (blue dashed line) and LQU (red line) with initial electron–proton states (8) for different values of α. For the separable initial state ($\alpha = 0$, first panel), both measures correctly begin at zero, confirming the absence of quantum correlations in the product state $|\uparrow_e\downarrow_p\rangle$. This panel shows characteristic oscillations of correlations with decreasing amplitude, emerging at $Gt > 0$, indicating periodic revivals of correlations during the dynamics. This revival can originate from the hyperfine interactions, which periodically re-align the electron and proton spins, partially restoring correlations. The second panel ($\alpha = \pi/3$) exhibits a weaker oscillatory behavior in agreement with the ESD but the LQU exhibited a smooth decay without the ESD. These oscillations reflect the exchange of spin excitations between the electron and proton, a hallmark of the Lindblad dynamics where unitary evolution dominates at short times. Notably, the LQU is more robust than concurrence, as it captures correlations even in separable states. In the third panel, corresponding to the initial maximally entanglement state with $\alpha = \frac{\pi}{4}$, the character exhibits a qualitatively distinct behavior. Unlike the other cases, neither measure begins at its maximal value, reflecting the presence of initial maximal quantum correlations in the initial state, and the subsequent dynamics lack the clear oscillatory structure observed elsewhere. This deviation suggests that the Bell state represents a useful case in which the hyperfine interaction generates more intricate correlation dynamics, possibly due to the balanced weighting between its constituent basis states. These results highlight the critical role of initial state preparation in shaping both the strength and temporal evolution of quantum correlations in the hydrogen hyperfine system.

It should also be noted that the behavior of the entanglement strongly depends on the choice of initial state. For the initial product states $\{|\uparrow_e\uparrow_p\rangle, |\downarrow_e\downarrow_p\rangle\}$, the concurrence remains identically zero at all times, indicating the complete absence of entanglement generation.

In the case of the initial product states $\{|\uparrow_e\uparrow_p\rangle, |\downarrow_e\downarrow_p\rangle\}$, the corresponding elements of the density matrix are given by

$$\rho_{11}(t) = \tfrac{1}{4} + \tfrac{1}{2}e^{-2\gamma t} + \tfrac{1}{4}e^{-4\gamma t}, \tag{19}$$

$$\rho_{22}(t) = \rho_{33}(t) = \tfrac{1}{4} - \tfrac{1}{4}e^{-4\gamma t}, \tag{20}$$

$$\rho_{44}(t) = \tfrac{1}{4} - \tfrac{1}{2}e^{-2\gamma t} + \tfrac{1}{4}e^{-4\gamma t}, \tag{21}$$

$$\rho_{ij}(t) = 0, \quad \text{for } i \neq j. \tag{22}$$

These solutions show that the concurrence remains identically zero for all times, confirming the complete absence of entanglement generation in this configuration. In contrast, for initial states $\{|\uparrow_e\downarrow_p\rangle, |\downarrow_e\uparrow_p\rangle\}$, the system exhibits a rich dynamical behavior characterized by oscillatory entanglement dynamics. These states show sudden-birth and sudden-death entanglement phenomena over time. This oscillatory behavior arises because of the coherent exchange interactions governed by the Hamiltonian of the hyperfine structure, which effectively couples the spin degrees of freedom of the electron and the proton. As a result, the interplay between unitary evolution and dissipative effects gives rise to non-trivial temporal patterns in the entanglement dynamics. The results obtained here are relevant for quantum information processing, as they quantify how quantum correlations, such as concurrence and local quantum uncertainty, evolve under decoherence. Understanding these dynamics is essential for the preparation, manipulation, and preservation of spin-based qubits in atomic systems. Our approach thus provides a framework for exploring strategies to protect quantum correlations against environmental noise, with potential applications in quantum computation, communication, and sensing.

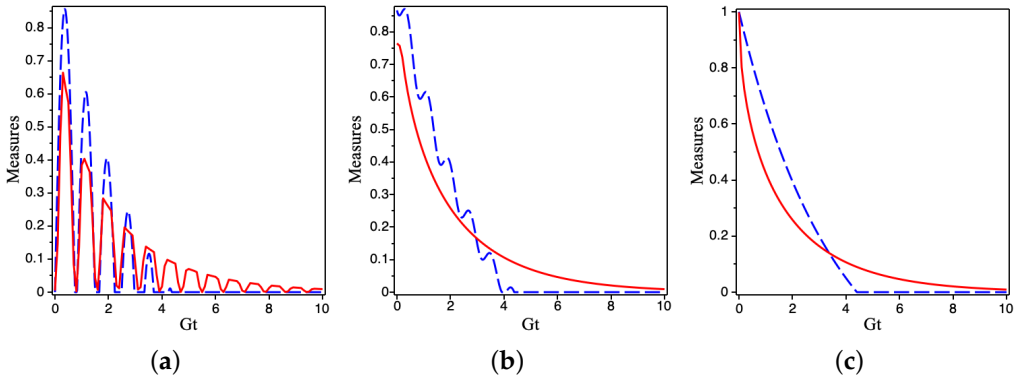

Figure 2. Time evolution of the measures (concurrence and LQU) as a function of time t for different coherent initial hyperfine states $\cos(\alpha)\,|\uparrow_e\downarrow_p\rangle + \sin(\alpha)\,|\downarrow_e\uparrow_p\rangle$. (**a**) is for the initial separate state $|\uparrow_e\downarrow_p\rangle$ ($\alpha = 0$); (**b**) is for initial coherent state $\alpha = \frac{\pi}{3}$; and (**c**) is for the initial maximally entangled state $\alpha = \frac{\pi}{4}$. For $\gamma = 0.1G$, the blue dashed line represents the concurrence, while the red solid line represents the LQU.

Although our analysis focuses on spin-flip (relaxation/excitation) processes, the qualitative trend of concurrence decaying faster than LQU is expected to hold for a broad class of Markovian noise channels. Quantitative aspects, such as decay rates and oscillation amplitudes, may vary depending on the particular decoherence model considered. Previous studies have confirmed similar qualitative behavior in spin-based systems under different types of noise [50,55,56]. This observation indicates that the main conclusions regarding the relative robustness of quantum correlations are largely model-independent and generally applicable to realistic open quantum systems.

The theoretical model presented here finds direct correspondence with experimental systems that manipulate hyperfine interactions in atomic and molecular settings. In particular, the ground-state hyperfine structure of hydrogen has been precisely measured using Ramsey spectroscopy, achieving a determination of the hyperfine interval with an uncertainty of 85 Hz [57]. These measurements are crucial for testing quantum electrodynamics predictions and provide a foundation for applications in quantum information processing. Furthermore, trapped-ion systems, such as those utilizing $^{171}Yb^{+}$ ions, have demonstrated exceptional coherence times exceeding 10 min in hyperfine qubits [58]. These long-lived qubits are ideal candidates for implementing quantum memories and processing units, aligning well with the dynamics described in our model.

Additionally, advancements in quantum networks have been achieved through high-fidelity quantum logic gates using trapped-ion hyperfine qubits, with fidelities reaching 99.9% [59]. These developments underscore the practical applicability of hyperfine interactions in scalable quantum computing architectures. Collectively, these experimental achievements not only validate the theoretical framework employed in this study but also pave the way for future investigations into the interplay between entanglement, local quantum uncertainty, and decoherence in systems governed by hyperfine interactions.

5. Conclusions

This study explored quantum correlations, including entanglement and quantum discord, within the hydrogen atom's hyperfine structure, a fundamental and experimentally accessible system in quantum mechanics, using the Lindblad master equation to model its dynamics as an open quantum system influenced by environmental interactions. By examining various initial states, particularly coherent superpositions of hyperfine states, we analyzed the temporal evolution of two key measures: concurrence, which quantified entanglement, and local quantum uncertainty (LQU), a broader indicator of quantum correlations. Our investigation yielded several significant findings. A primary outcome was the observed robustness of LQU in scenarios where entanglement, as measured by concurrence, dissipated due to environmental decoherence. Entanglement proved highly sensitive, exhibiting sudden death under intense dissipative conditions, whereas LQU demonstrated greater resilience, decaying gradually rather than abruptly. We have shown that the hyperfine structure of the hydrogen atom served as an effective platform for studying quantum correlations and decoherence, providing a controlled and analytically tractable framework. Moreover, the insights derived from this atomic system offered valuable perspectives on quantum correlation dynamics, potentially guiding advancements in quantum information processing tasks, where preserving quantum correlations in noisy environments was essential. The study establishes a clear connection between the dynamics of quantum correlations and fundamental physical parameters, shedding light on how non-classical features emerge in the evolution of hydrogen atoms. The findings deepen our understanding of quantum behavior in atomic systems and suggest the possibility of experimental observation in controlled laboratory environments. Ultimately, this work opens new perspectives on the role of quantum information in atomic physics. Future research could focus on experimental realizations, refined theoretical models, and applications of these insights to related systems, potentially advancing the development of quantum technologies based on atomic-scale platforms.

Author Contributions: Writing—original draft, K.B. and S.B.; writing—review and editing, K.B. and S.B. All authors have read and agreed to the published version of the manuscript.

Funding: This work was supported and funded by the Deanship of Scientific Research at Imam Mohammad Ibn Saud Islamic University (IMSIU) (grant number IMSIU-DDRSP2503).

Data Availability Statement: The original contributions presented in this study are included in the article. Further inquiries can be directed to the corresponding author.

Conflicts of Interest: The authors declare no conflict of interest.

References

1. Zoller, P.; Beth, T.; Binosi, D.; Blatt, R.; Briegel, H.; Bruss, D.; Calarco, T.; Cirac, J.I.; Deutsch, D.; Eisert, J.; et al. Quantum information processing and communication. *Eur. Phys. J. D* **2005**, *36*, 203–228. [CrossRef]
2. Bennett, C.H.; DiVincenzo, D.P.; Smolin, J.A.; Wootters, W.K. Mixed-state entanglement and quantum error correction. *Phys. Rev. A* **1996**, *54*, 3824–3851. [CrossRef]

3. Horodecki, R.; Horodecki, P.; Horodecki, M.; Horodecki, K. Quantum Entanglement. *Rev. Mod. Phys.* **2009**, *81*, 865–942. [CrossRef]
4. Petz, D. *Quantum Information Theory and Quantum Statistics*; Springer: Berlin/Heidelberg, Germany, 2008. [CrossRef]
5. Wootters, W.K. Entanglement of Formation of an Arbitrary State of Two Qubits. *Phys. Rev. Lett.* **1998**, *80*, 2245–2248. [CrossRef]
6. Modi, K.; Brodutch, A.; Cable, H.; Paterek, T.; Vedral, V. The classical-quantum boundary for correlations: Discord and related measures. *Rev. Mod. Phys.* **2012**, *84*, 1655–1707. [CrossRef]
7. Vedral, V.; Plenio, M.B.; Rippin, M.A.; Knight, P.L. Quantifying Entanglement. *Phys. Rev. Lett.* **1997**, *78*, 2275–2279. [CrossRef]
8. Vidal, G.; Werner, R.F. Computable measure of entanglement. *Phys. Rev. A* **2002**, *65*, 032314. [CrossRef]
9. Ollivier, H.; Zurek, W.H. Quantum Discord: A Measure of the Quantumness of Correlations. *Phys. Rev. Lett.* **2001**, *88*, 017901. [CrossRef]
10. Hu, M.L.; Hu, X.; Wang, J.; Peng, Y.; Zhang, Y.R.; Fan, H. Quantum coherence and geometric quantum discord. *Phys. Rep.* **2018**, *762*, 1–100. [CrossRef]
11. Maleki, Y.; Zheltikov, A.M. Linear Entropy of Multiqutrit Nonorthogonal States. *Opt. Express* **2019**, *27*, 8291–8307. [CrossRef]
12. Bosma, A. 21-cm line studies of spiral galaxies. I-Observations of the galaxies NGC 5033, 3198, 5055, 2841, and 7331. II-The distribution and kinematics of neutral hydrogen in spiral galaxies of various morphological types. *Astronom. J.* **1981**, *86*, 1791–1824. [CrossRef]
13. Furlanetto, S.R.; Oh, S.P.; Briggs, F.H. Cosmology at low frequencies: The 21cm transition and the high-redshift Universe. *Phys. Rep.* **2006**, *433*, 181–301. [CrossRef]
14. Yang, Q.; Dong, S. Probing dark matter axions using the hyperfine structure splitting of hydrogen atoms. *Phys. Lett. B* **2023**, *843*, 138004. [CrossRef]
15. Vessot, R.F.C.; Levine, M.W.; Mattison, E.M.; Blomberg, E.L.; Hoffman, T.E.; Nystrom, G.U.; Farrel, B.F.; Decher, R.; Eby, P.B.; Baugher, C.R.; et al. Test of Relativistic Gravitation with a Space-Borne Hydrogen Maser. *Phys. Rev. Lett.* **1980**, *45*, 2081–2084. [CrossRef]
16. Diermaier, M.; Jepsen, C.B.; Kolbinger, B.; Malbrunot, C.; Massiczek, O.; Sauerzopf, C.; Simon, M.C.; Zmeskal, J.; Widmann, E. In-beam measurement of the hydrogen hyperfine splitting and prospects for antihydrogen spectroscopy. *Nat. Commun.* **2017**, *8*, 15749. [CrossRef]
17. Kuroda, N.; Ulmer, S.; Murtagh, D.J.; Gorp, S.V.; Nagata, Y.; Diermaier, M.; Federmann, S.; Leali, M.; Malbrunot, C.; Mascagna, V.; et al. A source of antihydrogen for in-flight hyperfine spectroscopy. *Nat. Commun.* **2014**, *5*, 3089. [CrossRef]
18. Christensen, J.E.; Hucul, D.; Campbell, W.C.; Hudson, E.R. High-fidelity manipulation of a qubit enabled by a manufactured nucleus. *npj Quantum Inf.* **2020**, *6*, 35. [CrossRef]
19. Chae, E.; Choi, J.; Kim, J. An elementary review on basic principles and developments of qubits for quantum computing. *Nano Converg.* **2024**, *11*, 11. [CrossRef]
20. Acharya, R.; Abanin, D.A.; Aghababaie-Beni, L.; Aleiner, I.; Andersen, T.I.; Ansmann, M.; Arute, F.; Arya, K.; Asfaw, A.; Google Quantum AI; et al. Quantum error correction below the surface code threshold. *Nature* **2024**, *638*, 920–926. [CrossRef]
21. Niu, S.; Todri-Sanial, A.; Bronn, N.T. Multi-qubit dynamical decoupling for enhanced crosstalk suppression. *Quantum Sci. Technol.* **2024**, *9*, 045003. [CrossRef]
22. Veroni, S.; Müller, M.; Giudice, G. Optimized measurement-free and fault-tolerant quantum error correction for neutral atoms. *Phys. Rev. Res.* **2024**, *6*, 043253. [CrossRef]
23. Yang, X.; Long, X.; Liu, R.; Tang, K.; Zhai, Y.; Nie, X.; Xin, T.; Li, J.; Lu, D. Control-enhanced non-Markovian quantum metrology. *Commun. Phys.* **2024**, *7*, 282. [CrossRef]
24. Bellomo, B.; Lo Franco, R.; Compagno, G. Non-Markovian effects on the dynamics of entanglement. *Phys. Rev. Lett.* **2007**, *99*, 160502. [CrossRef]
25. Wang, B.; Xu, Z.Y.; Chen, Z.Q.; Feng, M. Non-Markovian effect on the quantum discord. *Phys. Rev. A* **2010**, *81*, 014101. [CrossRef]
26. Maniscalco, S.; Francica, F.; Zaffino, R.L.; Lo Gullo, N.; Plastina, F. Protecting Entanglement via the Quantum Zeno Effect. *Phys. Rev. Lett.* **2008**, *100*, 090503. [CrossRef] [PubMed]
27. Francica, F.; Plastina, F.; Maniscalco, S. Quantum Zeno and anti-Zeno effects on quantum and classical correlations. *Phys. Rev. A* **2010**, *82*, 052118. [CrossRef]
28. Carvalho, A.R.R.; Hope, J.J. Stabilizing entanglement by quantum-jump-based feedback. *Phys. Rev. A* **2007**, *76*, 010301. [CrossRef]
29. Root, D. Quantum Technologies in the Context of Climate Change: Emphasizing Sustainability in a Responsible Innovation Approach to Quantum Innovation. *NanoEthics* **2025**, *19*, 4. [CrossRef]
30. Fogedby, H.C. Field-theoretical approach to open quantum systems and the Lindblad equation. *Phys. Rev. A* **2022**, *106*, 022205. [CrossRef]
31. Makhlin, Y. Nonlocal Properties of Two-Qubit Gates and Mixed States, and the Optimization of Quantum Computations. *Quantum Inf. Process.* **2002**, *1*, 243–252. [CrossRef]

32. Li, M.; Wang, W.; Zhang, X.; Wang, J.; Li, L.; Shen, S. Regression of Concurrence via Local Unitary Invariants. *Entropy* **2024**, *26*, 917. [CrossRef]
33. Landau, L.; Lifshitz, E. *The Basic Concepts of Quantum Mechanics*, 3rd ed.; Elsevier: Oxford, UK, 1977; pp. 1–24. [CrossRef]
34. Demtröder, W. *Atoms, Molecules and Photons*; Springer: Berlin/Heidelberg, Germany, 2010; Volume 3, pp. 383–420. [CrossRef]
35. Pethick, C.J.; Smith, H. *Bose–Einstein Condensation in Dilute Gases*; Cambridge University Press: Cambridge, UK, 2008. [CrossRef]
36. Maleki, Y.; Sheludiakov, S.; Khmelenko, V.V.; Scully, M.O.; Lee, D.M.; Zheltikov, A.M. Natural and magnetically induced entanglement of hyperfine-structure states in atomic hydrogen. *Phys. Rev. A* **2021**, *103*, 052804. [CrossRef]
37. Nathan, F.; Rudner, M.S. Universal Lindblad equation for open quantum systems. *Phys. Rev. B* **2020**, *102*, 115109. [CrossRef]
38. Manzano, D. A short introduction to the Lindblad master equation. *AIP Adv.* **2020**, *10*, 025106. [CrossRef]
39. Budini, A.A. Lindblad rate equations. *Phys. Rev. A* **2006**, *74*, 053815. [CrossRef]
40. Hu, M.L.; Xi, X.Q.; Lian, H.L. Thermal and phase decoherence effects on entanglement dynamics of the quantum spin systems. *Phys. B Condens. Matter* **2009**, *404*, 3499–3506. [CrossRef]
41. Kraus, B.; Büchler, H.P.; Diehl, S.; Kantian, A.; Micheli, A.; Zoller, P. Preparation of entangled states by quantum Markov processes. *Phys. Rev. A* **2008**, *78*, 042307. [CrossRef]
42. Wootters, W.K. Entanglement of formation and concurrence. *Quantum Inf. Comput.* **2001**, *1*, 27–44. [CrossRef]
43. Walborn, S.; Souto Ribeiro, P.; Davidovich, L.; Mintert, F.; Buchleitner, A. Experimental determination of entanglement with a single measurement. *Nature* **2006**, *440*, 1022–1024. [CrossRef] [PubMed]
44. Bougouffa, S.; Hindi, A. Entanglement dynamics of a bipartite system in squeezed vacuum reservoirs. *Phys. Scr.* **2011**, *T143*, 175503. [CrossRef]
45. Aloufi, K.; Bougouffa, S.; Ficek, Z. Dynamics of entangled states in a correlated reservoir. *Phys. Scr.* **2014**, *90*, 074020. [CrossRef]
46. Bougouffa, S.; Ficek, Z. Entanglement transfer between bipartite systems. *Phys. Scr.* **2012**, *T147*, 014005. [CrossRef]
47. Bougouffa, S. Entanglement dynamics of two-bipartite system under the influence of dissipative environments. *Opt. Commun.* **2010**, *283*, 2989–2996. [CrossRef]
48. Algarni, M.; Berrada, K.; Abdel-Khalek, S.; Eleuch, H. Parity deformed tavis-cummings model: Entanglement, parameter estimation and statistical properties. *Mathematics* **2022**, *10*, 3051. [CrossRef]
49. Aldaghfag, S.A.; Berrada, K.; Abdel-Khalek, S. Entanglement and photon statistics of two dipole–dipole coupled superconducting qubits with Kerr-like nonlinearities. *Results Phys.* **2020**, *16*, 102978. [CrossRef]
50. Girolami, D.; Tufarelli, T.; Adesso, G. Characterizing Nonclassical Correlations via Local Quantum Uncertainty. *Phys. Rev. Lett.* **2013**, *110*, 240402. [CrossRef]
51. Coles, P.J.; Colbeck, R.; Yu, L.; Zwolak, M. Uncertainty Relations from Simple Entropic Properties. *Phys. Rev. Lett.* **2012**, *108*, 210405. [CrossRef] [PubMed]
52. Dakić, B.; Vedral, V.; Brukner, Č. Necessary and Sufficient Condition for Nonzero Quantum Discord. *Phys. Rev. Lett.* **2010**, *105*, 190502. [CrossRef]
53. Piani, M. Problem with geometric discord. *Phys. Rev. A* **2012**, *86*, 034101. [CrossRef]
54. Chang, L.; Luo, S. Remedying the local ancilla problem with geometric discord. *Phys. Rev. A* **2013**, *87*, 062303. [CrossRef]
55. Fanchini, F.F.; Cornelio, M.F.; de Oliveira, M.C.; Caldeira, A.O. Conservation law for distributed entanglement of formation and quantum discord. *Phys. Rev. A* **2010**, *81*, 052107. [CrossRef]
56. Girolami, D.; Adesso, G. Observable measure of bipartite quantum correlations. *Phys. Rev. Lett.* **2012**, *108*, 150403. [CrossRef] [PubMed]
57. Bullis, R.; Rasor, C.; Tavis, W.; Johnson, S.; Weiss, M.; Yost, D. Ramsey Spectroscopy of the $2S_{1/2}$ Hyperfine Interval in Atomic Hydrogen. *Phys. Rev. Lett.* **2023**, *130*, 203001. [CrossRef]
58. Wang, Y.; Um, M.; Zhang, J.; An, S.; Lyu, M.; Zhang, J.N.; Duan, L.M.; Yum, D.; Kim, K. Single-qubit quantum memory exceeding ten-minute coherence time. *Nat. Photonics* **2017**, *11*, 646–650. [CrossRef]
59. Ballance, C.; Harty, T.; Linke, N.; Sepiol, M.; Lucas, D. High-Fidelity Quantum Logic Gates Using Trapped-Ion Hyperfine Qubits. *Phys. Rev. Lett.* **2016**, *117*, 060504. [CrossRef] [PubMed]